JOURNAL OF MATERIALS SCIENCE 24 (1989) 3213–3220

Interface analysis of Si–C–O fibre/magnesium aluminosilicate matrix composites

MING Y. CHEN
Air Force Wright Aeronautical Laboratories, Wright-Patterson Air Force Base, Dayton, Ohio 45433-6533, USA

J. M. BATTISON, TAI-IL MAH
Universal Energy Systems Inc., 4401 Dayton-Xenia Road, Dayton, Ohio 45432, USA

Interface characteristics of Si–C–O (Nicalon^R) fibre-reinforced glass ceramic matrix composites were studied using scanning Auger microscopy (SAM). Composites with and without the cation additions of Ba, Nb, Zr, Li and Li–Zr–Nb to the magnesium aluminosilicate (MAS) matrix were fractured *in situ* under ultrahigh vacuum. SAM depth profiles and flexural strength results showed the compositional effects of the additives in the fibre–matrix interface region.

1. Introduction

Ceramic–ceramic composites offer a potential use in turbine engine applications with higher operating temperatures than existing refractory alloys. They are investigated in the area of high-strength retention and good oxidation resistance while providing a less brittle fracture mode than monolithic ceramics. The research activities in SiC/glass-ceramic composites have received special attention in recent years. Studies on Si–C–O/lithium aluminosilicate (LAS) composites [1] have demonstrated their high strength and toughness at high temperatures ($\sim 1000^\circ$ C). Reactions at the fibre–matrix interface appear to have significant effects on the overall mechanical properties of the composite. Formation of a carbon-rich layer at the fibre–matrix interface has been observed in composites which show high toughness; while brittle composites have shown little or no carbon-rich layer [2]. Degradation reactions such as oxidation of the reinforcing fibres during processing or subsequent annealing in an oxidizing environment, could certainly have a detrimental effect on the composite properties.

Alkoxide-derived magnesium aluminosilicate (MAS) glass-ceramic composites with Si–C–O fibre reinforcement have been developed in recent years [3]. Unlike the LAS matrix composites, these composites require no further heat treatment after fabrication to achieve a desired degree of crystallinity. In this paper, studies were done on SiC fibre-reinforced composites with and without the addition of cation dopants, such as Zr, Nb, Li, Ba and Li + Zr + Nb(LZN) to the MAS matrix. The effects of the matrix additives on the fibre–matrix interface and their subsequent effect on the mechanical performance of the composites were investigated. Three-point flexural strength as well as interfacial analysis of the composites will be presented.

2. Experimental procedure

Six matrix materials were synthesized by hydrolitic decomposition of metal alkoxides. This method has proved to be an effective way to achieve high purity and homogeneity of the mixed oxides. The matrix compositions are as follows:

$$\begin{aligned}
\text{MAS} &= 2MgO\text{–}2Al_2O_3\text{–}5SiO_2 \\
\text{BaMAS} &= 3\,\text{wt}\%\ BaO + \text{MAS} \\
\text{ZrMAS} &= 4\,\text{wt}\%\ ZrO_2 + \text{MAS} \\
\text{NbMAS} &= 5\,\text{wt}\%\ Nb_2O_5 + \text{MAS} \\
\text{LiMAS} &= 1\,\text{wt}\%\ Li_2O + \text{MAS} \\
\text{LZN} &= 2\,\text{wt}\%\ Li_2O + 4\,\text{wt}\%\ ZrO_2 \\
&\quad + 5\,\text{wt}\%\ Nb_2O_5 + MgO\text{–}Al_2O_3\text{–}5SiO_2
\end{aligned}$$

The composite processing procedure was similar to that of Hermes and Mazdiyasni [3]. Each matrix material was calcined and incorporated in a slurry composed of water and Rhoplex^R binder. Ceramic grade Nicalon^R fibre was desized, infiltrated with slurry, wound on a mandrel to the appropriate width and then allowed to air dry. After drying, suitable widths were cut perpendicular to the fibre direction and stacked uniaxially in a Grafoil^R lined graphite die. All hot-pressing was done at 1300° C $\pm$ 10° C for 15 min at 17.2 MPa (2500 p.s.i.) in vacuum. Binder burnout was achieved *in situ* at $\sim 600^\circ$ C.

After the hot-pressing, sample surfaces were ground with 600 grit SiC paper to remove Grafoil^R from the sample and sectioned into bend bars of dimensions 1.250 in. × 0.125 in. × 0.05 in. (approximately 3.18 cm × 0.318 cm × 0.128 cm). The X-ray analysis was done on ground sample surfaces, and perpendicular cross-sections were made to determine the fibre–matrix ratio. Transmission electron microscopic specimens (BaMAS, LZN) were prepared by coring 3 mm rods perpendicular to the fibre direction. The rods were cut to $\sim$0.015 in. ($\sim$0.038 cm) depths parallel to the fibre direction and hand ground to $\sim$0.005 in. ($\sim$0.013 cm) thick. Final thinning was achieved by ion milling in argon for $\sim$20 h.

0022–2461/89 $03.00 + .12

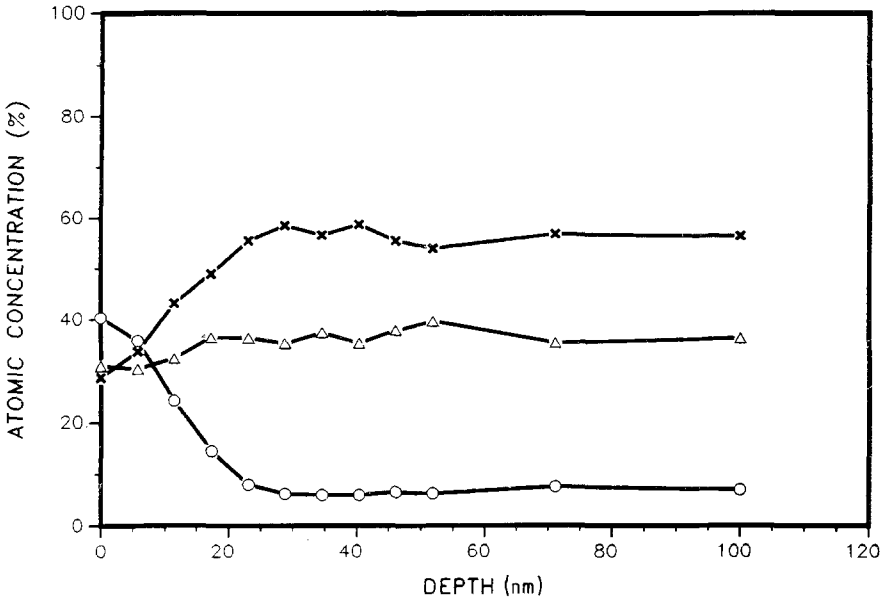

Figure 1 Depth profile for a flame-desized Nicalon fibre. (△) Si, (×) C, (○) O.

The interface analyses were performed utilizing a Perkin–Elmer Model 595 scanning auger microprobe combined with argon-ion bombardment profiling. The base vacuum pressures during analyses were in the range of 5×10^{-9} to 3×10^{-10} torr. The argon-ion beam was generated by a differentially pumped mini-beam ion gun. The base and sputtering pressures in the analysis chamber were 3×10^{-8} and 1×10^{-4} torr, respectively. An *in situ* fracture attachment allowed the composite to be fractured parallel to its fibre direction inside the vacuum chamber. The samples were held at approximately 30° angle from the electron beam to avoid charging. The sputtering rate was calibrated using a 100 nm thick Ta_2O_5/Ta specimen and the rate is $\sim 1.7\,nm\,min^{-1}$.

The electron probe voltage of 3 and 5 keV was used to generate the Auger spectra. The ion-beam voltage was held at 4 keV for depth profiling. Auger spectra of the freshly generated fibre–matrix interface were obtained and analysed. Additionally, elemental distributions perpendicular to the interface region were also measured.

3. Results

The X-ray analysis and flexural results are shown in Table I. The LZN-doped composites had the highest strength compared to the other composites. The cordierite phase was found in all except the LZN-doped composites.

A typical depth profile for flame-desized Nicalon fibres (Fig. 1) indicates the presence of a thin oxygen-rich layer (~ 6 nm) on the fibre surface. Note that the as-received Nicalon fibres came in tows each having ~ 500 fibres. The bulk concentration and fibre diameter were reported to be different from fibre to fibre within the same tow [2]. Similar variations in fibre concentration were also observed in this study. Based on several profile results, the bulk atomic concentration of the fibre consists of 36 to 44% Si, 46 to 57% C and 5 to 18% O. A representative example of the composite fracture surface for the MAS as well as for all the doped composites is shown in Fig. 2. Auger analysis and depth profiling were performed on the fibre regions and also on the matrix-trough regions to give chemical information at the interface. All the depth profiles for the doped and undoped MAS matrix composites show the presence of a carbon-rich layer at the interface. The profile results are detailed as follows.

The Auger spectrum for a fibre surface in the Nicalon/MAS composite at a depth of 21 nm (Fig. 3) indicated the presence of aluminium in addition to silicon, carbon and oxygen. It was observed that all the doped composites also showed evidence of aluminium in the fibre. The Auger spectrum for the trough area after a sputtering of 50 nm (Fig. 4) showed the presence of magnesium and aluminium as well as silicon, carbon and oxygen.

A typical depth profile for the Nicalon/MAS composite, shown in Fig. 5, indicates a carbon-rich layer of approximately 25 nm at the fibre region of the interface. The thickness of the carbon-rich layer on the fibre side can be estimated more consistently from sample to sample. By contrast, it was difficult to measure the carbon thickness on the matrix region due to a more complex chemistry and a very gradual change in the carbon concentration with depth. The fibre bulk concentration was reached at approximately 60 nm. At a depth of 160 nm into the trough, the bulk

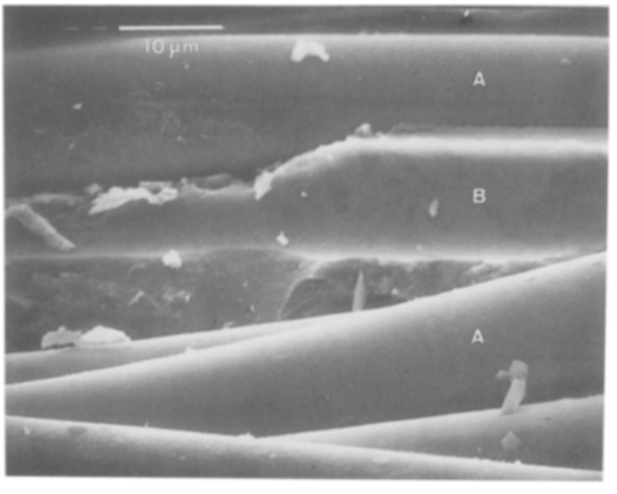

Figure 2 Micrograph of a typical composite fracture surface: A, fibre; B, trough.

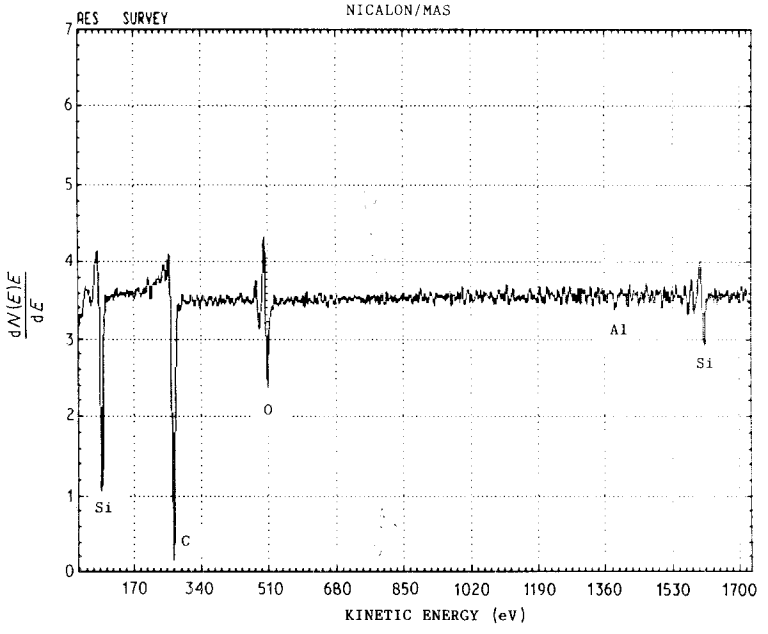

Figure 3 Auger spectrum of the Nicalon fibre surface in MAS composite; surface with 21 nm removed.

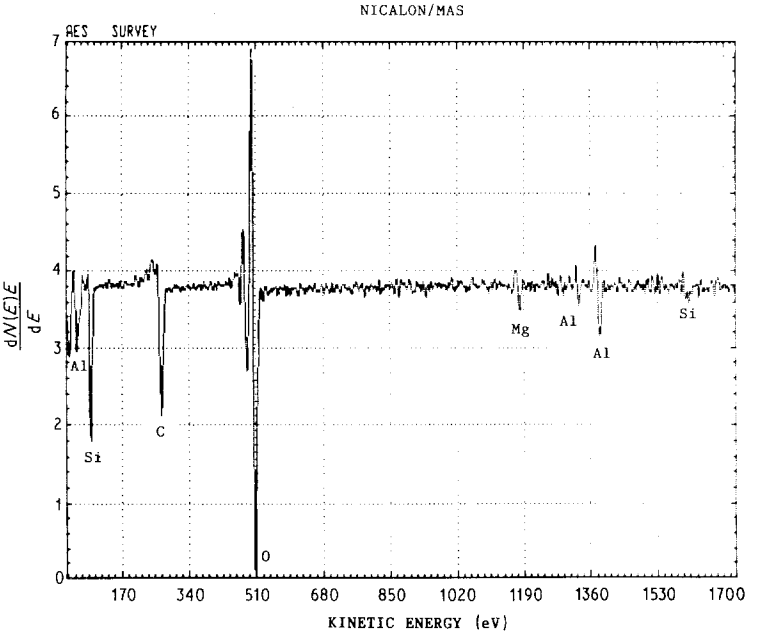

Figure 4 Auger spectrum of a trough region in MAS composite; surface with 50 nm removed.

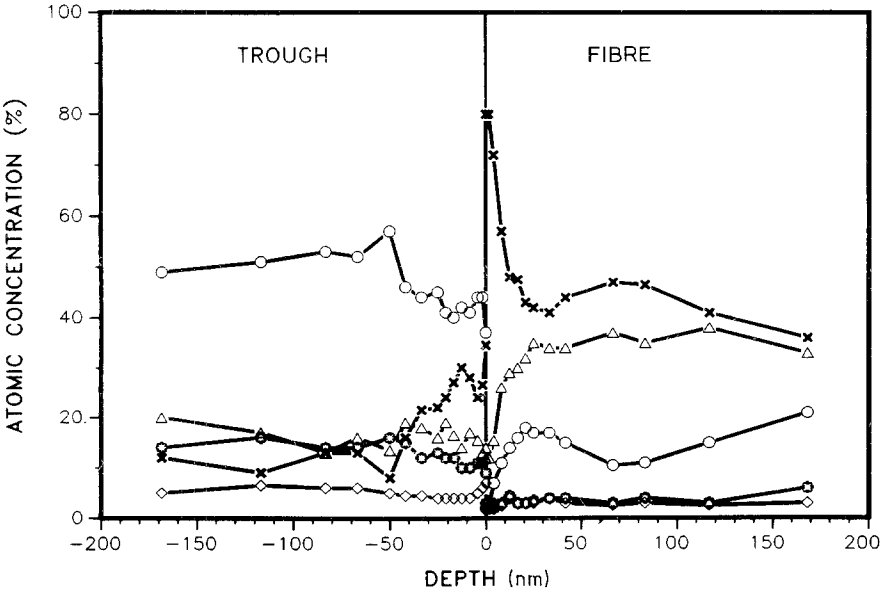

Figure 5 Depth profile for Nicalon/MAS composite. (△) Si, (×) C, (○) O, (◇) Mg, (☆) Al.

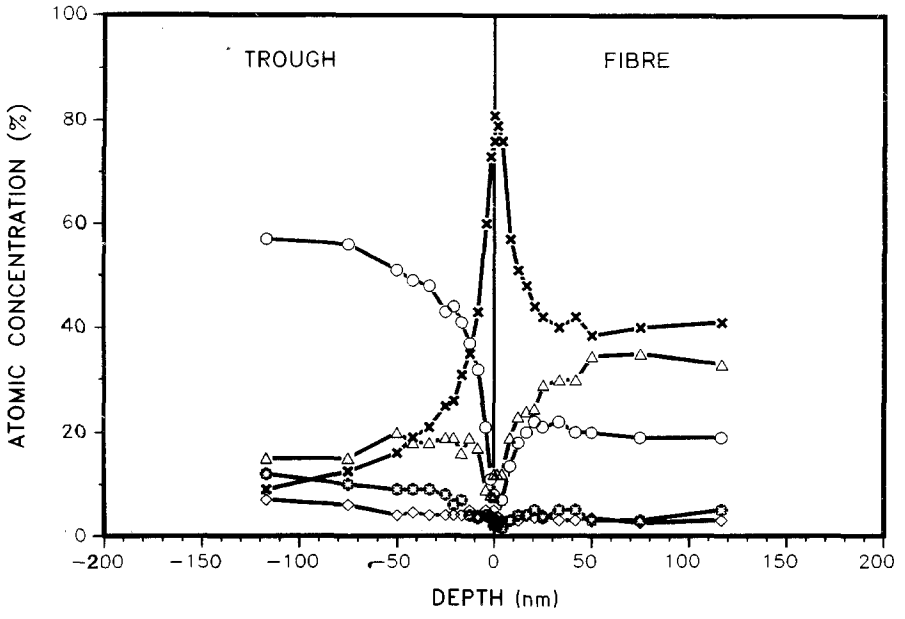

Figure 6 Depth profile for Nicalon/ZrMAS composite; for key, see Fig. 5.

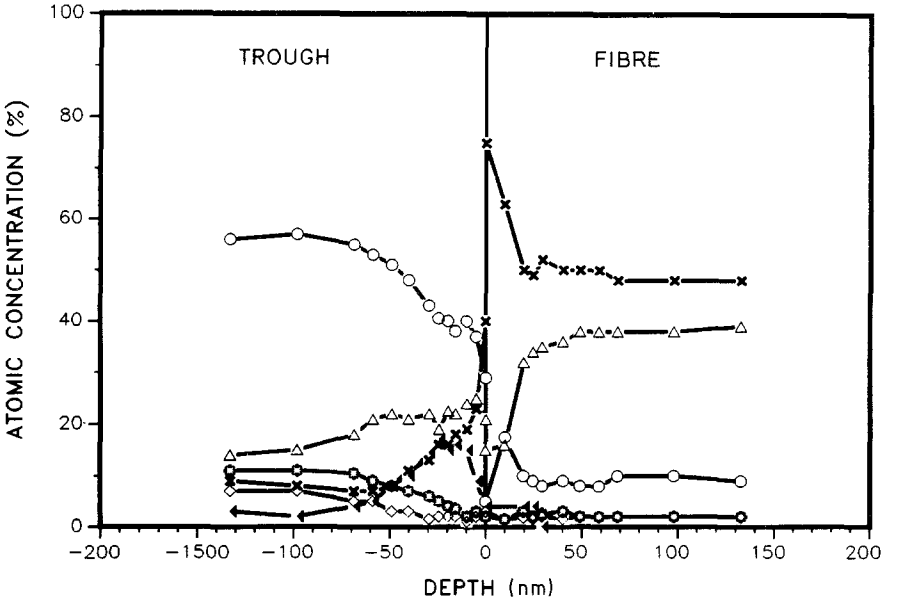

Figure 7 Depth profile for Nicalon/NbMAS composite; for main key, see Fig. 5; (◀) Nb.

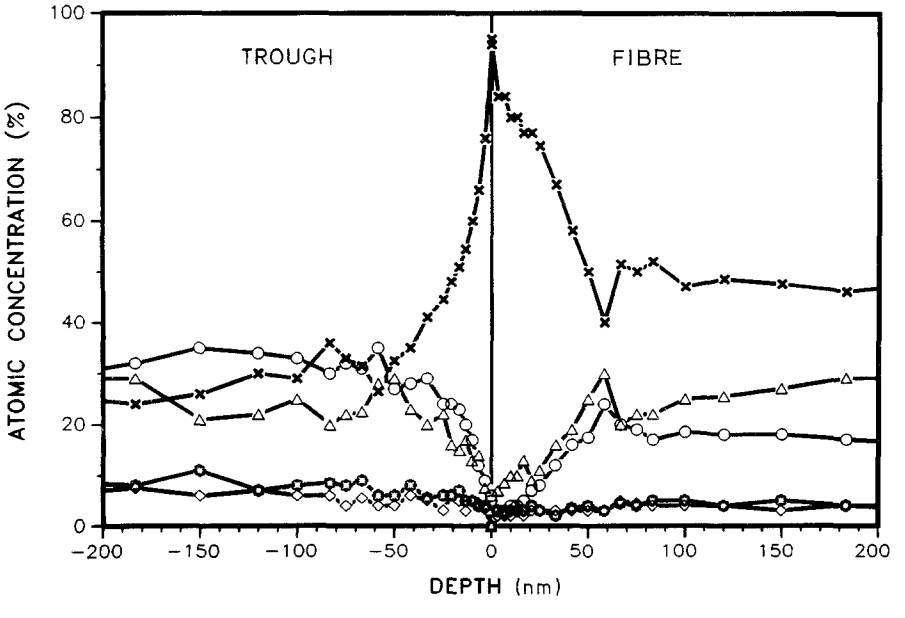

Figure 8 Depth profile for Nicalon/LiMAS composite; for key see Fig. 5.

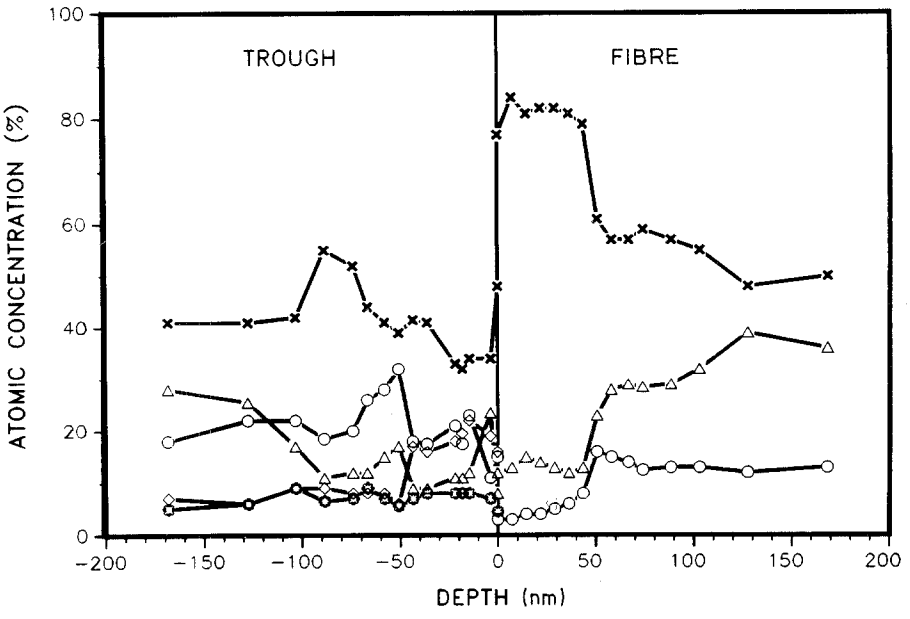

Figure 9 Depth profile for Nicalon/LiZrMAS composite. (△) Si, (x) C, (○) O, (◇) Nb, (☆) Al.

matrix composition was approached except that traces of carbon were still detected.

The zirconia-doped composite showed an overall similar depth profile with a 33 nm thick carbon-rich layer at the fibre (Fig. 6). In the matrix region, a trace of zirconium was detected.

The depth profile for the niobium-doped composite (Fig. 7) indicated a thinner carbon-rich layer at the interface (22.5 nm). Traces of niobium were detected at a depth of 24.5 nm into the fibre (confirmed from Auger spectrum). Higher niobium concentrations were found in the trough very close to the interface. At a depth of 15 to 50 nm into the trough region, the ratio of niobium to carbon approached unity, suggesting the formation of NbC. The carbon concentration generally decreased gradually to ~ 10 at % at 130 nm in depth into the trough. However, there was one case in which the carbon still remained relatively high (~ 30 at %) at this depth.

For the Li-doped composite (Fig. 8), the carbon-rich layer on the fibre was considerably thicker (~ 58 nm thick) than all the previous matrix compositions. The carbon concentration also remained very high (50 at %) at 230 nm into the trough.

The thickness of the carbon-rich layer on the fibre surface of LZN composites varied considerably from fibre to fibre (36, 51 to 74 nm). Traces of niobium (< 1 at %) were detected at the surface of the fibre (Fig. 9). A high niobium concentration was observed at 50 nm into the matrix. The carbon concentrations remained quite high (~ 40 at %) at 130 nm into most trough regions, except one region, at which the carbon (~ 20 to 23%) was lower than the oxygen concentration from surface to 130 nm in depth. This depth profile result is consistent with the TEM result (Fig. 10). As indicated in this micrograph, the niobium was found to have formed a layer of NbC particles with a thickness of ~ 20 to 50 nm.

The transmission electron micrograph for the barium-doped composite indicated a carbon-rich layer with a thickness ~ 33 to 47 nm at the fibre–matrix interface (Fig. 11). This was consistent with the depth-profile result, shown in Fig. 12, in which the thickness of the carbon layer on the fibre side was ~ 40 nm.

4. Discussion

The as-received Nicalon fibres were all flame desized prior to matrix infiltration. The surfaces of these fibres were found to be covered with an oxide layer.

TABLE I Results of flexural strength and phase identification

	Flexural strength*		Standard deviation		Fibre volume (%)	Phases present†
	(MPa)	(10^3 p.s.i.)	(MPa)	(10^3 p.s.i.)		
MAS	310	45	69	10	42	Cordierite
BMAS	386	56	62	9	45	Cordierite, mullite
NMAS	269	39	62	9	47	Cordierite, NbC
ZMAS	379	55	48	7	44	Cordierite, spinel‡
LMAS	386	56	30	4.4	45	Cordierite, β-spodumene, spinel
LZN	690	100	34	5	45	β-spodumene

*Three-point bend test, average of nine bars, 0.0508 mm min^{-1} cross-head speed.
† X-ray diffraction.
‡ Also traces of unknown peaks.

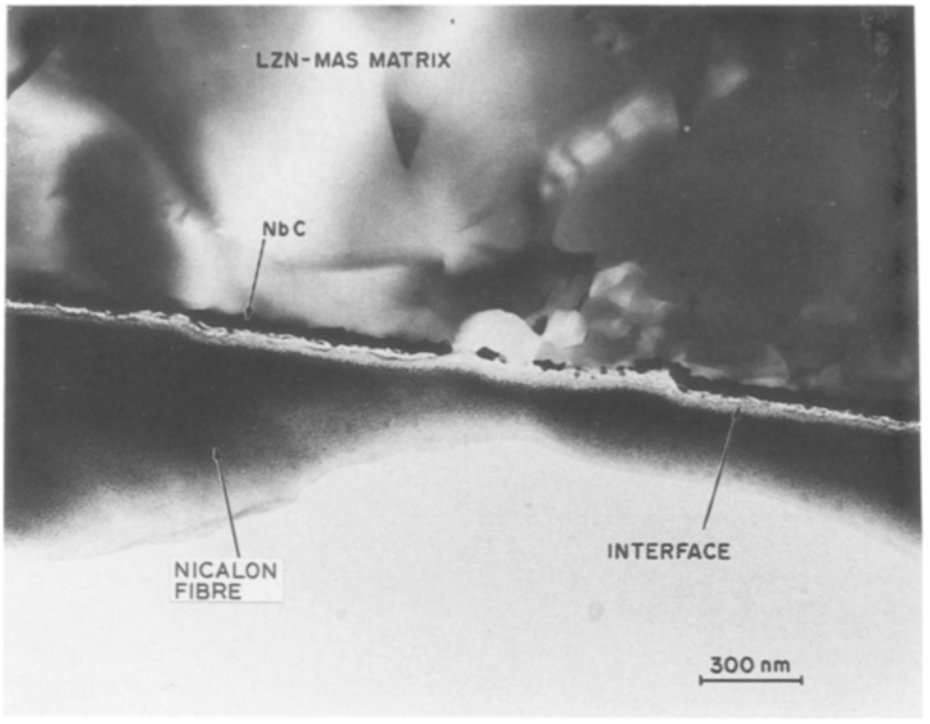

Figure 10 Transmission electron micrograph of Nicalon/LiZrNb-MAS composite.

However, analyses on fibres from either pure or doped MAS composites all indicated the presence of carbon-rich layers with varying thicknesses. The shapes of the carbon Auger peak (272 eV) for the as-fractured fibre and trough surfaces both resembled the shape of a graphite instead of carbon in a silicon carbide [4]. Knowing that there was originally no carbon on the flame-desized fibre surfaces and that the source of carbon could only arise from the bulk of fibres (assuming complete binder burn-out), then the observed carbon layer at the interface after sintering is a result of fibre–matrix reactions during the composite processing. Similar observations of carbon-rich layers has been reported [2].

There are at least two major factors contributing to uncertainty in the depth profiles. Firstly, because the composites were fractured and analysed *in situ*, the sample surface is usually with very high roughness which has a substantial influence on depth resolution [5]. Therefore, optimum profiles could not be obtained. Secondly, another important factor is the preferential sputtering of some elements relative to the others. This could result in depth profiles showing higher concentrations of elements with higher atomic weights

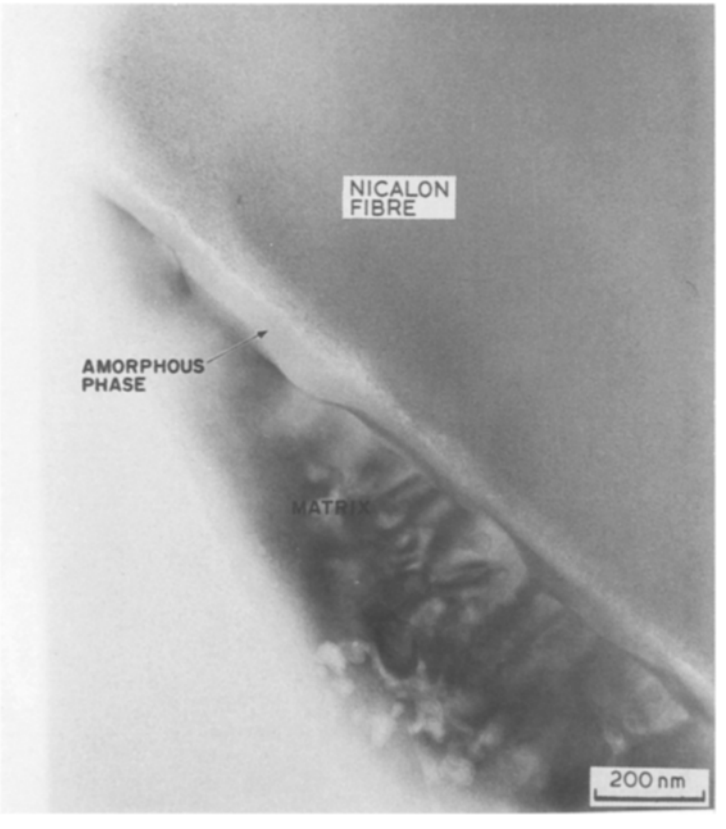

Figure 11 Transmission electron micrograph of Nicalon/BaMAS composite.

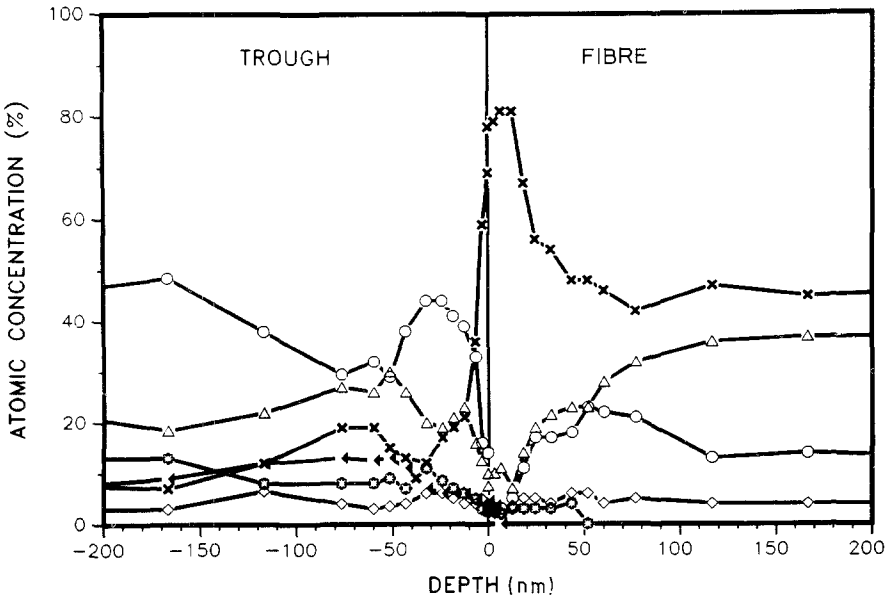

Figure 12 Depth profile for Nicalon/BaMAS composite; for main key, see Fig. 5, (◀) Ba.

which tend to have slower removal rates. The resulting depth profiles must be taken as approximations because of these contributing factors.

The depth profiles for the six composite systems and the TEM results have indicated that the transverse fracture occurred along the fibre–matrix interface region and consistently closer to the matrix than to the fibre. In the case of LZN-doped composites, the fracture took place between the NbC layer near the matrix and the carbon layer near the fibre. The cations (Al, Nb and Ba) diffused from the matrix toward the fibre while the carbon diffused from the fibre to the matrix. The observed carbon-rich layer at the fibre–matrix interface developed during the composite processing.

Because *in situ* fracture of the composites was near the matrix–carbon layer interface, the carbon layer on the trough surface tends to be very thin. Additionally, this thickness cannot be estimated consistently from one sample to another. Therefore, the carbon layer thickness on the fibre side of the interface is used to approximate the total carbon layer thickness. The average thickness of the carbon-rich layer on the fibre side of the interface compared to the ultimate flexural strength of the composites is summarized in Fig. 13. The ranges of thickness and strength variations are indicated at each point. Note that the LiZrNb-doped composite has a much higher flexural strength and a larger range of thickness variation than the other composites have. The large range of thickness variation for LiZrNb-doped composites may be attributed to the fact that *in situ* fracturing of the composite can occur anywhere along the carbon-rich interface from the matrix to the fibre. Therefore, a thicker interface tends to give a higher range of thickness variation. It appears from this figure that the composites with thicker carbon layers tend to also have higher flexural strengths. It is very likely that other differences exist between these composites in addition to the variation in the carbon thickness and that they could account for discrepancy in this figure (especially the lithium-doped composites). However, it appears from these results that the composite with the thickest carbon layer also had the highest strength (see Table I).

5. Conclusion

The fibre–matrix interface regions were found to be

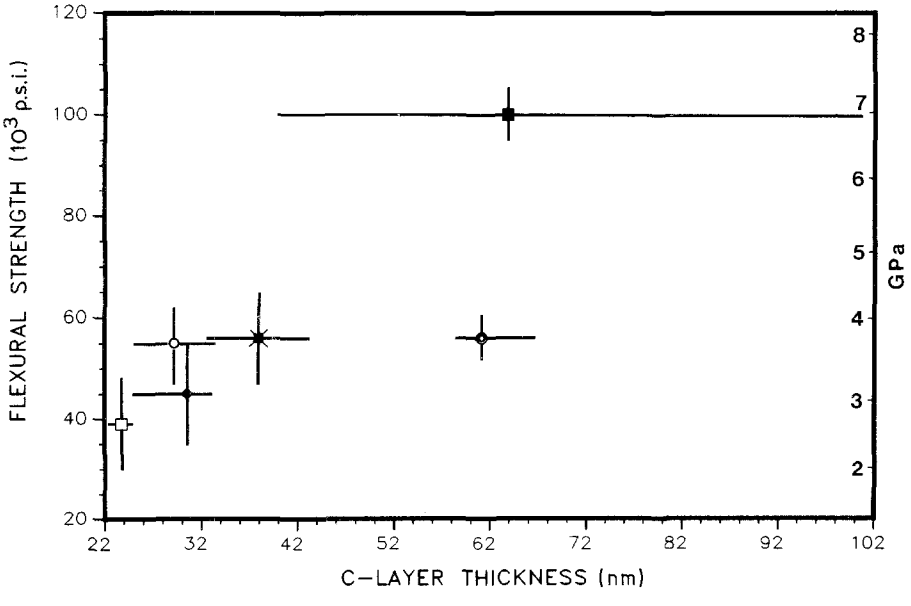

Figure 13 Average flexural strength plotted against thickness of the carbon-rich layer on the fibre surface. (◆) MAS, (◎) LiMAS, (x) BaMAS, (○) ZrMAS, (□) NbMAS, (■) LiZrNbMAS.

carbon rich for all six composite systems. Transverse fracture occurred very close to the matrix along the interface region. Aluminium, niobium and barium diffused from the matrix into the fibre while the carbon diffused from the fibre to a carbon-rich layer, and from there into the matrix. The thickness of the carbon-rich layer was greatest for LiZrNb-doped followed by lithium-doped, barium-doped, MAS, zirconium-doped and then niobium-doped composites. The ultimate flexural strength also followed a similar relationship. The composite with the thicker carbon-rich layer along the interface also had the higher flexural strength.

Acknowledgement

This work was sponsored in part by the Air Force Wright Aeronautical Laboratories, Materials Laboratory, Wright-Patterson Air Force Base, Contract number F33615-84-C-5116.

References

1. J. J. BRENNAN and K. M. PREWO, *J. Mater. Sci.* **17** (1982) 2371.
2. J. J. BRENNAN, "Additional Studies of SiC Fiber Reinforced Glass–Ceramic Matrix Composites", Annual Report R84-916018-4, ONR Contract N00014-82-C-0096, 1 April 1984.
3. E. E. HERMES and K. S. MAZDIYASNI, "Processing and Characterization of SiC Fiber Reinforced Magnesium Alumino Silicate Composites", NASA Conference Publication 2406 (1985) pp. 217–228.
4. K. MIYOSHI and D. H. BUCKLEY, "XPS, AES and Friction Studies of Single-Crystal Silicon Carbide", in "Applications of Surface Science", Vol. 10 (North-Holland, Amsterdam, 1982) pp. 357–76.
5. S. HOFMANN, J. ERLEWEIN and A. ZALAR, *Thin Solid Films* **43** (1977) 275.

Received 7 June
and accepted 21 October 1988